National Aeronautics and Space Administration

Multiscale Computer Simulation of Failure in Aerogels

Brian S. Good, Materials and Structures Division, NASA Glenn Research Center, Cleveland, Ohio

ABSTRACT

Aerogels have been of interest to the aerospace community primarily for their thermal properties, notably their low thermal conductivities. While such gels are typically fragile, recent advances in the application of conformal polymer layers to these gels has made them potentially useful as lightweight structural materials as well. We have previously performed computer simulations of aerogel thermal conductivity and tensile and compressive failure, with results that are in qualitative, and sometimes quantitative, agreement with experiment. However, recent experiments in our laboratory suggest that gels having similar densities may exhibit substantially different properties. In this work, we extend our original diffusion limited cluster aggregation (DLCA) model for gel structure to incorporate additional variation in DLCA simulation parameters, with the aim of producing DLCA clusters of similar densities that nevertheless have different fractal dimension and secondary particle coordination. We perform particle statics simulations of gel strain on these clusters, and consider the effects of differing DLCA simulation conditions, and the resultant differences in fractal dimension and coordination, on gel strain properties.

INTRODUCTION

Silica aerogels are low-density materials whose thermal properties have made them of ongoing interest for a wide variety of applications [1–3]. While pristine gels are fragile, polymer coating gels can greatly improve their strength while minimally impacting their insulating properties [4].

In order to provide a microscopic understanding of the mechanical behavior of the gels, and to provide a predictive tool of use in their further development, we have constructed a multiscale model for the tensile and compressive failure of silica aerogels. The model is based on computer simulations using a modified diffusion-limited cluster aggregation (DLCA) scheme to generate model gel structures, and combines atomistic molecular statics calculations whose results are abstracted into input for larger-scale particle statics failure simulations.

In previous related work we have found our methodology produces qualitatively reasonable strain and failure behavior, the details of which depend on model gel density [5]. However, researchers in our laboratory have found that aerogels having the same density may nonetheless exhibit different thermal and mechanical properties [4]. Therefore we have revisited our early exploratory work in an attempt to determine whether varying the DLCA simulation parameters other than density can reproduce this observed behavior.

AEROGEL STRUCTURE

Aerogels exhibit a ropy, low-density morphology that displays three levels of structure. X-ray and neutron probes suggest that the gels consist of disordered aggregates of connected fractal clusters, with fractal behavior evident over a limited range of length scales [6–9]. Fractal dimensions of 1.7 to 1.9 at small length scales have been observed in low-density colloidal materials [10].

The smallest structural detail is the so-called “primary” particle, a few nanometers in diameter, consisting of approximately fully dense amorphous silica. Primary particles aggregate into “secondary” particles an order of magnitude larger, and typically somewhat lower in density. Secondary particles, in turn, are connected via interparticle bridges, and form the observed porous structure that may range from a “pearl-necklace” network, to a denser, more highly coordinated structure. It has been reported that gels having the same density may nevertheless exhibit differing properties.

Figure 1.—Silica aerogels. 0.016 g/cm³ (left), 0.450 g/cm³ (right).

STRUCTURAL MODEL

Our structural model considers only secondary particles, which are assumed to be homogeneous; their detailed structure and any internal degrees of freedom are not considered here. Secondary particles sizes are uniform, or are chosen at random from log-normal or truncated Gaussian distributions, with a mean radius of 15 nm.

Model gel structures are produced by DLCA computer simulation [11]:

- 5000 single-particle clusters (solitary secondary particles) are distributed at random without overlap in a computational cell whose size determines the density. Cluster aggregation proceeds via repeated move/merge cycles:
- A cluster to be moved is chosen at random with probability $P_i = (m_i / m_0)\alpha$ where m_i and m_0 are the masses of the moving cluster, and the lightest cluster in the cell, respectively, and a is a scaling parameter.
- The moving cluster is given a small “diffusive” displacement in a random direction. If one or more collisions occur, the colliding clusters are merged into a single cluster at the point of collision.
- The simulation terminates when only a single cluster remains.

The following DLCA parameters are varied in an attempt to determine the sensitivity of fractal dimension, coordination, and strain energetics on simulation conditions:

- Cluster diffusive step size (2, 3, 5, 7.5, and 15 nm)
- Particle size distribution method and width (uniform size, log normal, or truncated Gaussian distributions with widths σ = 3, 4, 7.5,10, and 15 nm)
- Cluster move probability scaling exponent ($\alpha = 0.25$, 0.5, 0.75, and 1.0)

A default parameter set is defined, with stepsize = 1 nm, $\alpha = 0.5$, and uniform particle size.

STRUCTURAL MODEL RESULTS—FRACTAL DIMENSION

DLCA simulations were performed for a range of densities (0.0377, 0.0651, 0.127, and 0.302 g/cm³, designated low, medium-low, medium-high, and high density, respectively) that are typical of observed gel densities [3]. Final states of representative low- and high-density computational cells are presented in figures 2(a) and (b).

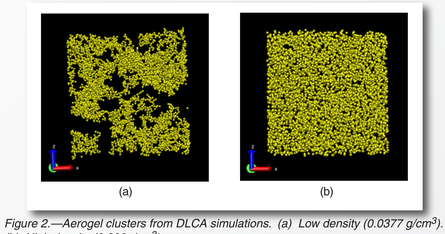

Figure 2.—Aerogel clusters from DLCA simulations. (a) Low density (0.0377 g/cm³). (b) High density (0.302g/cm³).

Fractal dimensions of clusters have been computed from the mass scaling. The variation in mass scaling with simulation parameters is shown in figures 3 (a) to (e). The density (fig. 3 (a)) appears to be the dominant factor in determining the fractal dimension. There are two distinct scaling regimes; at small r, fractal dimensions in order of increasing density are 1.80,1.95, 2.15, and 2.51, while at large r, the values are 2.71, 2.82, 2.87, and 2.87, indicating near-compact scaling. The small-r low-density value is consistent with experiment.

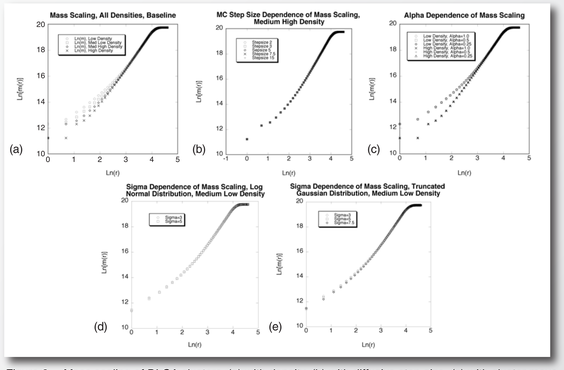

Figure 3.—Mass scaling of DLCA clusters. (a) with density. (b) with diffusive step size, (c) with cluster move probability scaling exponent, and (d) to (e) with particle distribution method (LN = log normal, TG = truncated Gaussian), and width. (b) and (c) are for medium high density, 0.127 g/cm³; (d) and (e) are for medium-low density, 0.0651 g/cm³.

The diffusive step size (fig. 3 (b)) has little effect on the fractal dimension, even when varied by almost an order of magnitude. Similar behavior is observed for the cluster move probability scaling exponent (fig. 3 (c)), and the particles size distribution method and distribution width (figs. 3 (d) to (e)).

The average coordination (defined in this context as the number of neighboring secondary particles in actual contact with a given particle) is found to behave similarly to the mass scaling behavior; again, the density dominates, with other parameters having little effect.

CLUSTER FAILURE MODEL

Interparticle bridges are typically smaller in diameter than the particles they connect; we therefore assume that failure occurs only through the stretching and breaking of bridges. We examine the strain energetics of the bridges via atomistic simulation and use the results to construct a simplified potential that describes interactions among the secondary particles.

ATOMISTIC SIMULATION OF BRIDGE STRAIN

We assume that interparticle interactions are described by a radial potential. The form of this potential is obtained from molecular statics simulation on an amorphous silica computational cell consisting of two representative spherical secondary particles connected by a bridge. (In previous work, we have included an additional angular component in the potential; with a radial component alone, failure is found to be too ductile. In the interest of computational efficiency, we have deleted with angular term for this work, which is intended to be qualitative in nature.)

Atomic interactions are described by a Rappe-Goddard potential (eq. 1), which consists of a short-range Morse component and a Coulomb component. Morse parameters are listed in table 1.

The bridges are repeatedly strained axially in tension by a small amount, with the atoms in the hemispheres on either end (furthest from the bridge) constrained to be rigid. The remainder of the atoms are allowed to relax between strains via molecular statics, where all relaxations proceed along the local energy gradient, and the total energy versus strain is recorded.

$$[1] \qquad V(r) = V_0\left[\exp(\gamma r_{ij}/r_0) - 2\exp(\gamma r_{ij}/2r_0)\right] + q_i q_j / r_{ij}$$

	V_0	r_0	γ
Si-Si	2.0537E–14	3.4103E–8	11.7139
Si-O	3.1957E–12	1.6148E–8	8.8022
O-O	3.7260E–14	3.7835E–8	10.4112

$q_{Si} = 1.22e$; $q_O = -0.61e$

Table 1.—Rappe-Goddard potential parameters

BRIDGE STRAIN RESULTS

A sequence of images from the bridge strain simulation are shown in figure 4, and bridge strain energy is shown in figure 5. While short-range phenomena indicative of the straining and breaking of smaller substructures are evident, the energy curve generally appears to resemble the Universal Binding Energy Relation of Rose, Ferrante and Smith [12], and, as such, can be fit to a Morse potential function. The function described here differs from the Morse function used in the atomistic simulations in that it represents the sum of atomic-scale interactions between two secondary particles; its range is much smaller, relative to secondary particle size, than an atomic Morse potential, for example, as used in the bridge strain energetics simulations.

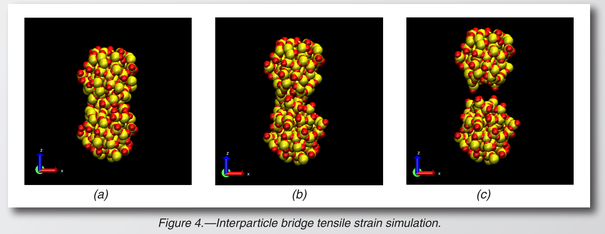

Figure 4.—Interparticle bridge tensile strain simulation.

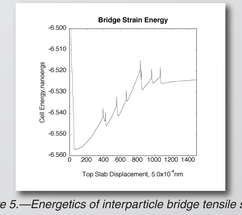

Figure 5.—Energetics of interparticle bridge tensile strain.

GEL CLUSTER STRAIN

Tensile strain is applied to DLCA clusters via a nanoscale particle statics approach. A displacement of 0.01 nm is applied to a rigid slab at the top of the cluster, and the remaining particles in the cluster are then relaxed along the local energy gradient using step sizes an order of magnitude smaller.

Initial and final states of two clusters, of densities 0. 0377 g/cm³ and 0.302 g/cm³, are shown in figures 6 (a) to (b). It can be seen that in both cases there is a tendency for chains of secondary particles to stretch in the direction of the strain before breaking. This tendency leads to fracture behavior that is too ductile; the tendency is considerably reduced when an angular term is added to the potential, and work is currently under way to expand these results using such a modified potential.

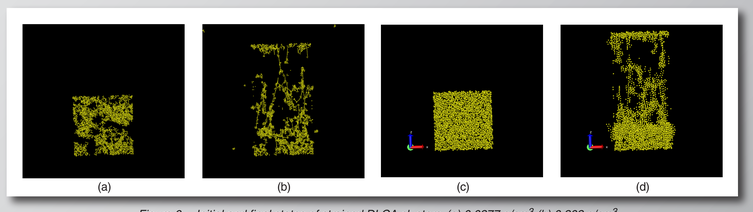

Figure 6.—Initial and final states of strained DLCA clusters. (a) 0.0377 g/cm³ (b) 0.302 g/cm³.

Because we do not expect fracture behavior to be correct in detail due to the absence of the angular term, we instead concentrate on the small-strain energy dependence. Energy versus slab displacement is shown in figures 7 (a) to (d). As with the fractal dimension, the density (a) is the dominant variable. Although the energy curves are quite noisy (additional runs, for the purpose of providing smoother curves via averaging, are under way), a simple linear fit to the lower portion of each curve provides qualitative information. The highest-density cluster is the stiffest, with the other three showing only small differences. There is no meaningful variation in energy with stepsize (b), alpha (c), and sigma (d).

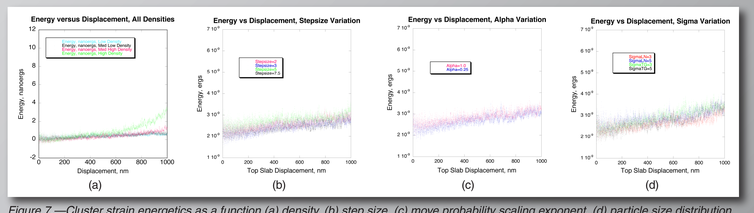

Figure 7.—Cluster strain energetics as a function (a) density, (b) step size, (c) move probability scaling exponent, (d) particle size distribution width. (b) to (d) are for medium highg density, 0.127 g/cm³.

CONCLUSIONS

We have performed computer simulations of the tensile strain and failure of silica aerogels, based on a multiscale model for cluster interactions, and a diffusion-limited cluster aggregation model for the gel structure. The simulations were carried out at levels of density typical of the densities of real aerogels. We find that the DLCA algorithm is surprisingly robust with respect to variation of simulation parameters. Over the ranges of parameters studied, only changes in density causes significant differences in cluster fractal dimension and energetics. Therefore we do not yet have a model that successfully explains differences in properties among clusters having the same density. It has been suggested that simple DLCA clusters exhibit particle chain structure that is too linear, and that loops are an important structural feature of real gels. Therefore we are modifying our DLCA code to allow for linear particle chain rotation and loop formation, in addition to the particle aggregation included in the current model. It may be that the degree of looping in clusters having the same density will yield different average coordinations, and different strain properties.

REFERENCES

1. N. Husing and U. Schubert, Angew. Chem. Int. Ed. 37, 22 (1998).
2. A. C. Pierre and G. M. Pajonk, Chem. Rev. 2002, 102, 4243 (2002).
3. J. L. Rousset, A. Boukenter, B. Champagnon, J. Dumas, E. Duval, J. F. Quinson and J. Serughetti, J. Phys.: Condens. Matter 2, 8445 (1990).
4. M. A. B. Meador, E. F. Fabrizio, F. Ilhan, A. Dass, G. Zhang, P. Vassilaras, J. C. Johnston and N. Leventis, Chem. Mater. 17, 1085 (2005).
5. B. Good, Mater. Res. Soc. Symp. Proc Vol. 978, 0978-GG05-03.
6. D. W. Schaeffer, J. E. Martin and K. D. Keefer, Phys. Rev. Lett. 56, 2199 (1986).
7. T. Freltoft, J. K. Kjems and S. K. Sinha, Phys. Rev. B 33, 269 (1986).
8. R. Vacher, T Woignier, J. Pelous and E. Courtens, Phys. Rev. B 37, 6500 (1988).
9. A. Hasmy, E. Anglaret, M. Foret, J. Pelous and R. Julien, Phys. Rev. B 50, 1305 (1994).
10. D. A. Weitz and M. Oliveria, Phys. Rev. Lett. 52, 1433 (1984).
11. P. Meakin, Phys. Rev. Lett. 51, 1119 (1983).
12. J. H. Rose, J. Ferrante and J. R. Smith, Phys. Rev. Lett. 47, 675 (1981).

P–11477–1
Mar 08